Graph Theoretical Generation and Analysis of Hydrogen-Bonded Structures with Applications to the Neutral and Protonated Water Cube and Dodecahedral Clusters

Shannon McDonald,[†] Lars Ojamäe,[‡] and Sherwin J. Singer*,[†]

Department of Chemistry, Ohio State University, Columbus, Ohio 43210, and Physical Chemistry, Arrhenius Laboratory, Stockholm University, S-106 91 Stockholm, Sweden

Received: December 1, 1997

Graph theoretical techniques are demonstrated to be of considerable use in the search for stable arrangements of water clusters. Inspired by the so-called "ice rules" that govern which hydrogen-bond networks are physically possible in the condensed phase, we use graphical techniques to generate a multitude of local minima of neutral and protonated water clusters using oriented graph theory. Efficient techniques to precisely enumerate all possible hydrogen-bonding topologies are presented. Empirical rules regarding favorable water neighbor geometries are developed that indicate which of the multitude of hydrogen-bonding topologies available to large water clathrates (e.g., 30 026 for $(H_2O)_{20}$) are likely to be the most stable structures. The cubic $(H_2O)_8$ and dodecahedral $(H_2O)_{20}$ clusters and their protonated analogues are treated as examples. In these structures every molecule is hydrogen bonded to three others, which leads to hydrogen-bonding topology fixing the cluster geometry. Graphical techniques can also be applied to geometrically irregular structures as well. The enumerated oriented graphs are used to generate initial guesses for optimization using various potential models. The hydrogen-bonding topology was found to have a significant effect on cluster stability, even though the total number of hydrogen bonds is conserved. For neutral clusters, the relationship between oriented graphs and local minima of several potential models appears to be one-to-one. The stability of the different topologies is rationalized primarily in terms of the number of nearest neighbor pairs that both have a free OH bond. This leads to the identification of water dodecahedra of greatest stability.

Considerable effort has been devoted to the theoretical prediction of the locally stable configurations of small water clusters, the identification of the global minimum from among the many local minima, and the experimental testing of these results.[1−40,80] The motivation for this intense interest is the need to accurately model water as a solvent for chemical processes, especially for modeling biochemical and environmental processes. The study of finite clusters provides a testing ground for detailed verification of models of water,[41−51] which can then be applied in bulk situations. The locally stable arrangements and thermal behavior of water clusters are also of fundamental intellectual interest, the main issues being the unusual properties of finite systems compared to the bulk and how the bulk limit is approached as cluster size tends toward macroscopic dimensions.[52−55]

Several attempts have been made to systematically generate the locally stable geometries of small water clusters and predict their relative energies. Tsai and Jordan have performed the most exhaustive searches using an eigenmode-following algorithm.[27−30] While of moderate computational cost for smaller clusters, the task of exhaustive enumeration of locally stable isomers rapidly increases in complexity with cluster size, not only because of the increasing cost of evaluating the potential and its derivatives but also because the number of local minima increases exponentially with cluster size. The purpose of this work is to provide some analytical guidance and theoretical understanding to complement previous numerical work. This guidance proves essential for the study of larger clusters, such as the $(H_2O)_{20}$ and $H^+(H_2O)_{20}$ cage structures. These structures are treated in this paper and are shown to possess tens of thousands of distinct (*not* symmetry-related) local minima. Candidates for the most stable of these structures are presented here.

The central physical assumption leading to an analytical method for enumeration of local structures is that each water molecule may participate in a maximum of two hydrogen bonds as a hydrogen donor and, through the two lone pairs, up to two hydrogen bonds as an acceptor. These ideas have been central in the literature on water and ice for many years.[56−58] Their expression for solid water structures are the so-called "ice rules" or "Bernal−Fowler" rules.[59,60] In the liquid phase, they motivate older flickering crystal theories[59] and more recent random network models for water. A hydronium ion can donate up to three hydrogen bonds. By inspection of the many published structures available for water clusters and bulk water, virtually all hydrogen bonds between water molecules can be assigned a direction, which we take to be from donor to acceptor. The one exception is symmetrical hydrogen bonds whose prototype is the $H_5O_2^+$ ion.[35,61] Structures with the excess proton in a symmetrical hydrogen bond can also be enumerated using graph theory by assigning either a nondirectional or empty bond to the unit carrying the excess charge.

When a water molecule participates in four (Figure 1a) or three (Figure 1b,c) hydrogen bonds, its position is fixed by those bonds and we expect only a single minimum energy position for that water molecule. In low-energy structures of small ($n \lesssim 25$) water clusters, four-coordinated waters are relatively rare,

[†] Ohio State University.
[‡] Stockholm University.

S1089-5639(98)00353-3 CCC: $15.00
Published on Web 04/04/1998

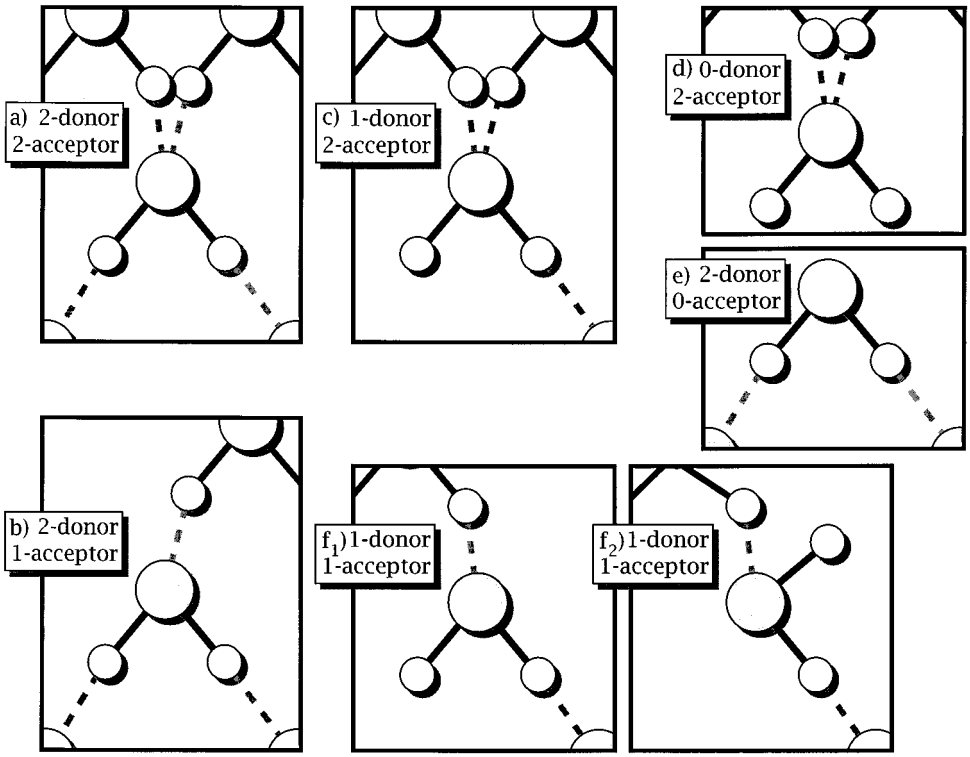

Figure 1. Depiction of a water molecule participating in (a) two hydrogen bonds as a donor and two as an acceptor, (b) two hydrogen bonds as a donor and one as an acceptor, (c) one hydrogen bond as a donor and two as an acceptor, (d) no hydrogen bonds as a donor and two as an acceptor, (e) two hydrogen bonds as a donor and none as an acceptor, and (f_1 and f_2) one hydrogen bond as a donor and one as an acceptor, showing the two possible orientations in the latter case.

occurring for example in multiple-cube structures, but three-coordination is quite common. A doubly-coordinated, double-acceptor or double-donor water (Figure 1d,e) may also be fixed by virtue of its hydrogen bonding to other waters. However, a double-coordinated, single-donor water should have at least two minimum energy positions (Figure 1f_1,f_2), according to which lone pair accepts an incoming hydrogen bond. Singly-bonded waters should be rather floppy.

The topology of hydrogen bonds in a water cluster is summarized by an oriented graph, that is, a set of vertices and at most one oriented line connecting each pair of vertices. This idea has been previously pursued by Radhakrishnan and Herndon.[62] They performed ab initio calculations for selected structures, based on oriented graphs, for clusters as large as the cyclic octamer. Radhakrishnan and Herndon then correlated their ab initio results with topological invariants of the oriented graphs. Our work is in that respect similar in spirit to that of Radhakrishnan and Herndon. In our work, new graph derivation methods for H-bonded clusters are presented, which allows us to tackle, in a systematic manner, much more complex structures, including a 20-member dodecahedral cage, where the enumeration problem has not previously been solved. We focus on structures in which the waters are minimally three-coordinate, so it is more likely that physical local potential energy minima are in one-to-one correspondence with oriented graphs. We also consider both neutral and protonated clusters, using the "OSS2" potential energy surface developed by Ojamäe, Shavitt, and Singer[63] and semiempirical PM3 calculations[64,65] to extend the description to protonated clusters. A trend we observe for clusters of 8 and 20 water molecules, namely destabilization of the cluster associated with adjacent double-donor or double-acceptor water molecules, was previously noted by Smith and Dang for $Cs^+(H_2O)_{20}$[22] and $(H_2O)_{20}$.[66]

Our working assumption is that, when the molecules are fixed by the hydrogen bonding arrangement, each local minimum of a water cluster corresponds to a single oriented graph. As discussed above, this occurs when the water molecules participate in two or more hydrogen bonds, except for the single-donor/single-acceptor case where two local minima would correspond to a single graph. For some water clusters, it appears that the relationship is also one-to-one, that for each oriented graph a corresponding-local minimum in found. For protonated water clusters, our experience is that not every graph has a corresponding local minimum. These conclusions may depend on the potential energy surface and skill in guessing initial geometries for optimization. When our working assumption is accurate, as would be expected for compact structures, oriented graphs provide a valuable enumeration of the local minima of water clusters. In this paper we discuss enumeration techniques (section I), cubic clusters of eight waters (section II), and dodecahedral cages of 20 waters (section III). We conclude with an assessment of the utility of graphical techniques for enumeration of water structures.

I. Enumeration Techniques

Enumeration techniques for oriented graphs were developed by Harary[67] with some specific formulas and methods for locally restricted graphs (as when ice rules are enforced) later offered by Harary and Palmer.[68,69] The general class of techniques without local constraints is based on a theorem by Polya and is described in several texts.[70−72] Polya's theorem gives us an upper bound to the number of hydrogen-bonding arrangements, since at this level the ice rules are not enforced.

Polya's theorem gives the total number of oriented graphs with m bonds based on the symmetry group of the vertices,[71] that is, the set of all permutations of the vertex labels that maintain the bonding arrangement. The symmetry group on

the vertices induces an isomorphic symmetry group on oriented bonds. Each member of the bond group must be resolved into independent cycles, from which a cycle index polynomial is generated. To enumerate oriented graphs, the appropriate cycle index polynomial is[67,68,71]

$$Z = \frac{1}{|G|}\sum_{i=1}^{|G|}\left(\prod_k b_{n_k}\right) \quad (1)$$

where the sum indexed by i is over all members of the group G of permutations on oriented bonds, the product indexed by k is over all pairs of converse cycles of group element i, and n_k is the length of cycle k or group element i. The converse of a cycle is the cycle generated by reversing every oriented bond. Self-converse cycles are not included in the cycle index polynomial.

We have determined the cycle index polynomials for a cube and dodecahedron appropriate for counting of oriented graphs:

$$Z_{\text{cube}} = {}^1/_{48}(b_1^{12} + 3b_2^4 + 6b_2^5 + 6b_1^2 b_2^5 + 4b_2^6 + 8b_3^4 + 12b_4^3 + 8b_6^2) \quad (2)$$

$$Z_{\text{dodec}} = {}^1/_{120}(b_1^{30} + 15b_1^2 b_2^{13} + 15b_2^{14} + b_2^{15} + 20b_3^{10} + 24b_5^6 + 20b_6^5 + 24b_{10}^3) \quad (3)$$

Polya's theorem relates the number of symmetry-distinct graphs with m oriented bonds to the coefficient of x^m in the polynomial obtained by replacing b_n with $1 + 2x^n$ in the cycle index polynomials. For the cube and dodecahedron, the results are

$$\text{cube:}\quad 1 + x + 10x^2 + 43x^3 + 188x^4 + 548x^5 + 1292x^6 + 2152x^7 + 2724x^8 + 2392x^9 + 1472x^{10} + 528x^{11} + 112x^{12} \quad (4)$$

$$\text{dodecahedron:}\quad 1 + x + 22x^2 + 287x^3 + 3755x^4 + 38160x^5 + 317548x^6 + 2172664x^7 + 12490998x^8 + 61049720x^9 + 256403818x^{10} + 932326512^{11} + 2952363660x^{12} + 8175660672x^{13} + 19855186704x^{14} + 42357535328x^{15} + 79420431072x^{16} + 130809856896x^{17} + 188947695352x^{18} + 238670498560x^{19} + 262537720524x^{20} + 250035717632x^{21} + 204574839040x^{22} + 142312814592x^{23} + 83015912504x^{24} + 39847592384x^{25} + 15326035968x^{26} + 4541038080x^{27} + 973086720x^{28} + 134217728x^{29} + 8948312x^{30} \quad (5)$$

To illustrate the significance of terms in the above equation, the final term indicates that there are 8 948 312 topologically distinct ways to arrange 30 oriented bonds on a dodecahedral graph. Some of these arrangements correspond to neutral clusters, some to an excess proton, and many, such as those in which a vertex has three incoming bonds, to hydrogen-bonding arrangements that are not physically realizable. The cycle index polynomials were easily generated from the permutation groups using a symbolic algebra program.[73]

Upon enforcement of local constraints—in this work, the ice rules—the enumeration problem becomes considerably more complex. Harary and Palmer[69] have given a procedure that is valid for local constraints. However, the algebra involved is too lengthy, even for machine evaluation (involving, e.g., manipulation of $\sim 120 \cdot 2^{30} \approx 10^{12}$ terms for the dodecahedron), and we were forced to develop a more efficient procedure.

Our graphical enumeration procedure for locally restricted graphs also rests upon representation of graphical configurations with polynomials. A factor of $\mu_i \nu_j x_{ij}$ in a term of the polynomial indicates a bond in which vertex i donates a hydrogen bond to j (i.e., an oriented bond pointing from i to j). All possible oriented graphs are generated by the polynomial

$$\prod_{\text{bond pairs ij}} (\mu_i \nu_j x_{ij} + \mu_j \nu_i x_{ji}) \quad (6)$$

Each factor $(\mu_i \nu_j x_{ij} + \mu_j \nu_i x_{ji})$ gives the two possible orientations at each bond pair. The above polynomial enumerates graphs in which each possible bond pair is occupied by an oriented bond. If unoccupied bonds are also to be included in the enumeration, then $(\mu_i \nu_j x_{ij} + \mu_j \nu_i x_{ji})$ is replaced with $(1 + \mu_i \nu_j x_{ij} + \mu_j \nu_i x_{ji})$.

Since the power of μ_i and ν_i in each term gives the number of outgoing and incoming bonds at vertex i, respectively, the ice rules for neutral clusters are enforced by annihilating an terms in eq 6 in which the power of μ_i or ν_i exceeds 2. For clusters containing a hydronium, one vertex is allowed to have three outgoing bonds.

So far, this procedure would enumerate many oriented graphs that are related to another by a symmetry operation. The next step would be a partition of the terms into equivalence classes, with members of each equivalence class related to each other by a permutation of the vertices. Selection of a single representative from each equivalence class completes the enumeration.

The number of terms in eq 6 makes the procedure, as described so far, prohibitively lengthy. However, it can be considerably shortened by annihilating all terms in violation of the ice rules or related to others by a symmetry operation after multiplication by each factor $(\mu_i \nu_j x_{ij} + \mu_j \nu_i x_{ji})$ [or $(1 + \mu_i \nu_j x_{ij} + \mu_j \nu_i x_{ji})$ if unoccupied bonds are allowed]. In words, the set of all graphs is incrementally constructed by decorating one bond at a time. If two partially constructed graphs are related to each other by a symmetry operation, they will give rise to the same set of fully occupied graphs, to within a symmetry operation, upon addition of more bonds. Therefore, only one of the partially constructed graphs related to each other by a symmetry operation need be retained at each stage. The same considerations apply to enforcement of the ice rules. If a partially constructed graph violates the ice rules, then all graphs made by adding more oriented bonds will also violate the ice rules. If we let A symbolize the operator which annihilates terms in violation of the ice rules or which are related to others by a symmetry operation, then symbolically we are stating that the left and right hand sides of the following equation are equivalent and that the right hand side is far more efficient to enumerate.

$$A\prod_{\text{bonds}} (\mu_i \nu_j x_{ij} + \mu_j \nu_i x_{ji}) = \ldots A\,(\mu_k \nu_l x_{kl} + \mu_l \nu_k x_{lk})\,A\,(\mu_i \nu_j x_{ij} + \mu_j \nu_i x_{ji}) \quad (7)$$

Later we shall see that the number of oriented graphs that satisfy the ice rules is roughly 10% of the total number of oriented graphs.

For the neutral and protonated water clusters considered in this work, each water molecule can be classed as single- or double-donors of hydrogen bonds and/or single- or double-acceptors of hydrogen bonds. A hydronium unit may also be a triple donor or zero-acceptor. With n_{bond} the number of

hydrogen bonds, n_O the number of oxygens, n_{proton} the number of *excess* protons, $n_H = 2n_O + n_{proton}$ the total number of hydrogens, m_H the number of hydrogens in hydronium units *not* participating in a hydrogen bond, m'_H the number of zero-acceptor neutral water units, n_{1D}, n_{2D}, ... the number of single-, double-, ... donors, and n_{0A}, n_{1A}, ... the number of zero-, single-, ... acceptors, then counting the number of bonds,

$$n_{1D} + 2n_{2D} + 3n_{3D} = n_{bond} \quad (8)$$

$$n_{1A} + 2n_{2A} = n_{bond} \quad (9)$$

oxygens,

$$n_{1D} + n_{2D} + n_{3D} = n_O \quad (10)$$

$$n_{0A} + n_{1A} + n_{2A} = n_O \quad (11)$$

and hydrogens,

$$2n_{1D} + 2n_{2D} + 3n_{3D} + m_H = n_H \quad (12)$$

$$3n_{0A} + 2n_{1A} + 2n_{2A} - m'_H = n_H \quad (13)$$

gives the relations

$$n_{0A} = n_{proton} + m'_H \quad (14)$$

$$n_{3D} = n_{proton} - m_H \quad (15)$$

$$n_{1A} = -2m'_H - n_{bond} + 2n_O - 2n_{proton} \quad (16)$$

$$n_{1D} = -m_H - n_{bond} + 2n_O + 2n_{proton} \quad (17)$$

$$n_{2A} = m'_H + n_{bond} - n_O + n_{proton} \quad (18)$$

$$n_{2D} = 2m_H + n_{bond} - n_O - 2n_{proton} \quad (19)$$

In the cubic and dodecahedral water clusters studied in this work, all waters and hydroniums are three-coordinate. In these cases, $n_{bond} = {}^3/_2 n_O$ and $m'_H = 0$, yielding the simplified relations

$$n_{0A} = n_{proton} \quad (20)$$

$$n_{3D} = n_{proton} - m_H \quad (21)$$

$$n_{1A} = {}^1/_2 n_O - 2n_{proton} \quad (22)$$

$$n_{1D} = -m_H + {}^1/_2 n_O + n_{proton} \quad (23)$$

$$n_{2A} = {}^1/_2 n_O + n_{proton} \quad (24)$$

$$n_{2D} = 2m_H + {}^1/_2 n_O - 2n_{proton} \quad (25)$$

II. Cubic $(H_2O)_8$ and $H^+(H_2O)_8$

The $(H_2O)_8$ cluster has recently been observed experimentally, and its cubic geometry confirmed by comparison with ab initio predictions.[51] For the eight 3-fold coordinated vertices of cubic $(H_2O)_8$, we have enumerated 14 oriented graphs. Initial guesses for the structures of $(H_2O)_8$ were generated from these graphs by placing oxygen vertices 2.8 Å apart, hydrogens participating in hydrogen bonds along the oxygen−oxygen bond, and unbonded hydrogens pointing radially outward from the center of the cube.[74] The structures were first annealed by Monte Carlo simulated annealing (only energy-lowering moves accepted, i.e., $T = 0$ K), followed by conjugate gradient refinement. The potential model was OSS2,[63] which can describe both neutral and protonated water clusters. Each initial guess optimized to a distinct locally stable structure. The oriented graphs and structures are depicted in Figure 2.

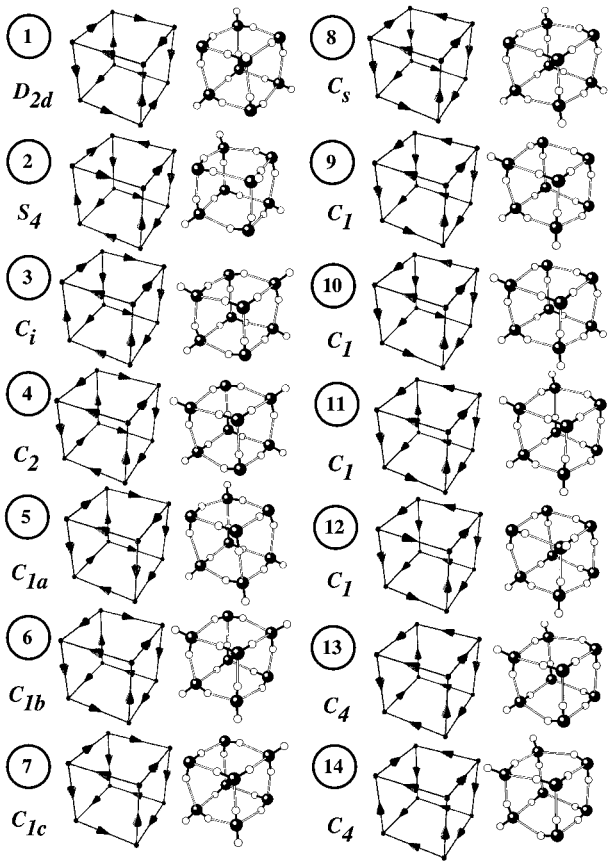

Figure 2. Oriented graphs and optimized structures for $(H_2O)_8$. The symmetry group of the graph is also indicated. The first eight structures were also described by Tsai and Jordan.[27] The three clusters of C_1 symmetry are labeled with an extra letter *a*, *b*, or *c* in accordance with Tsai and Jordan's notation.

Previously, local minima of cubic $(H_2O)_8$ were numerically enumerated by Tsai and Jordan[27] using a TIPS4P potential energy surface and an eigenmode-following surface walking algorithm.[28] We find that all of Tsai and Jordan's reported structures are in one-to-one correspondence with structures derived from oriented graphs. The remainder of the 14 local minima in Figure 2 are among the many local minima of higher energy that Tsai and Jordan found but did not report. A comparison of the energies of Tsai and Jordan's TIPS4P structures, MP2 calculations (with and without BSSE correction) at the TIPS4P geometries, and the OSS2 potential[63] is given in Figure 3. The OSS2 potential[63] follows the MP2 trend with greater accuracy than the TIPS4P potential.

It is of considerable interest to develop empirical correlations between hydrogen-bonding topology and cluster stability, providing guidance for further theoretical investigation and practical rules for predicting stable isomers. The relative energies of the $(H_2O)_8$ cube can apparently be described using very localized topological properties. The curve labeled "fit" in Figure 3 is

$$E(\mathrm{cm}^{-1}) = E(D_{2d}) + 17.7933 + 877.09n_{2D-2D} - 75.6473n_{4-ring} \quad (26)$$

where $E(D_{2d})$ is the energy of the D_{2d} structures, n_{2D-2D} is the

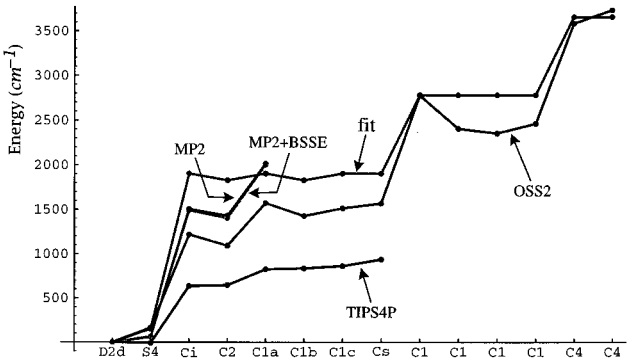

Figure 3. Energy differences of cubic $(H_2O)_8$ clusters from the energy of the D_{2d} structure. The plot includes structures calculated using the TIPS4P potential by Tsai and Jordan,[27] MP2 level ab initio energies calculated at the TIPS4P geometries also taken from the work of Tsai and Jordan,[27] (results with and without BSSE correction are almost indistinguishable on this plot), and energies calculated by us using the OSS2 potential.[63] Also shown is a fit (eq 26) to the relative energy of the structures based on two topological invariants, the number of nearest neighbor double-donors (or double-acceptors) and the number of four-member rings in which the hydrogen bonds all circulate in the same direction. The order of the structures corresponds to that in Figure 2.

number of nearest neighbor double-donors (according to the topological constraints given in eqs 20−25, $n_{2D-2D} = n_{2A-2A}$, the number of nearest neighbor double-acceptors), and n_{4-ring} is the number of four-membered rings in which all hydrogen bonds are oriented in the same direction. The above formula indicates that the relative energy of different hydrogen-bonding arrangements in $(H_2O)_8$ correlates most strongly with an effective repulsion associated with nearest neighbor double-donors or -acceptors. This repulsion may arise from the fact that for adjacent double-acceptors each water molecule has an unbound OH bond sticking out from the cluster. Repulsion between these positively charged H-atoms might play a role in destabilizing these neighbor pairs. Elucidating the physical mechanism behind these trends will be left to future theoretical investigations. In this context, note that Radhakrishnan and Herndon have previously developed correlations between the energies of water clusters and topological invariants.[62]

There are 11 oriented graphs with three outgoing lines at one vertex that correspond to protonated $H^+(H_2O)_8$ in which the excess proton associated with a single oxygen in a hydronium-like configuration (Figure 4). We could generate only six structures with hydronium-like protons from the 11 initial guesses corresponding to the oriented graphs. In some cases, initial guesses for one topological arrangement of $H^+(H_2O)_8$ optimized to a structure associated with another oriented graph. In other cases, optimization left the excess proton in an symmetrical $H_5O_2^+$-like bond. In one case, optimization led to an open, noncubic structure. Initial guesses were generated in the same manner as for the neutral cluster with two exceptions. Firstly, the H−O−H angles in the hydronium unit were opened up slightly. Secondly, we found that an initial bond length of 2.8 Å sometimes optimized to $H_5O_2^+$-like bonds in which the excess proton was roughly symmetrically placed between two oxygens. When this occurred, setting the initial bond length to a slightly larger value of 3.0 Å could force the excess proton to localize in a hydronium unit in some cases, while in others optimization still yielded an $H_5O_2^+$-like excess proton. It is possible that we could have found more structures with hydronium-like protons using more clever initial guesses for optimization or with a different potential energy model.

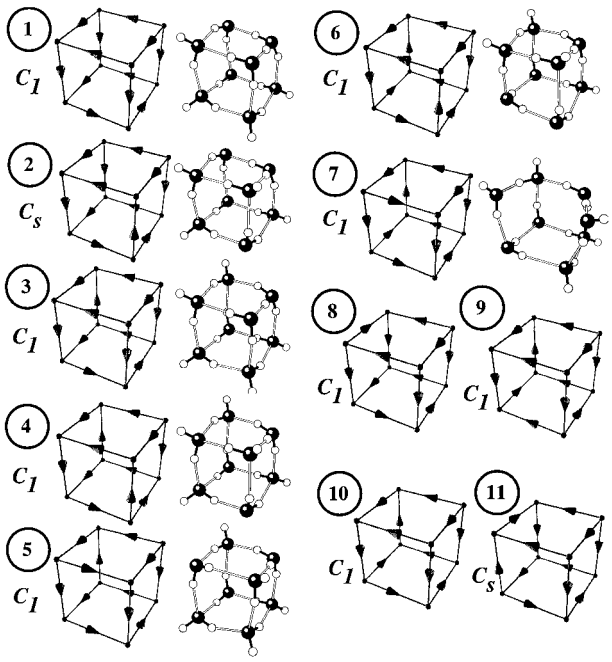

Figure 4. Oriented graphs and optimized structures for $H^+(H_2O)_8$ in which the excess proton is localized on one oxygen in a hydronium-like unit. The symmetry group of the graph is also indicated. We were only successful in optimizing initial guesses based on graphs **1**−**6** into structures corresponding to those graphs. Graph **7** optimized to the open structure shown above. Initial guesses based on graphs **8** and **9** optimized to the same structure as graph **1**. Initial guesses based on graphs **10** and **11** optimized to the same $H_5O_2^+$-like structures associated with graphs **2** and **1**, respectively, in Figure 5.

It occurred to us that long-range electrostatics might dominate the energetic trends in the protonated cluster. However, a crude estimate of charge−dipole couplings based on bond dipoles along each of the oriented edges revealed no difference among the 11 graphs (Figure 4) found for $H^+(H_2O)_8$. The energies of different hydrogen-bonding arrangements of protonated $H^+(H_2O)_8$ do seem to be correlated with local topological features, just like their neutral counterparts. Compared to the neutral cluster, there is an additional topological invariant based on nearest neighbor sitings available to describe the number of double-donor or double-acceptor waters near the hydronium. In addition to n_{2D-2D} and n_{4-ring}, which have the same meaning as in eq 26, we chose n_{2A-Hyd}, the number of double-acceptors adjacent to the hydronium, to be the additional parameter in the following fit

$$E(\mathrm{cm}^{-1}) = E(\mathbf{1}) - 504.465 + 1107.89n_{2D-2D} + 506.759n_{2A-Htd} - 183.799n_{4-ring} \quad (27)$$

where $E(\mathbf{1})$ is the energy of structure **1** in Figure 4. The energy cost of adjacent double-donors and gain for circulating rings is similar to that in the neutral cluster. In addition, there is a preference for double-donors to be adjacent to the hydronium.

The symmetry-distinct oriented graphs that correspond to protonated $H^+(H_2O)_8$ in which the excess proton resides in a symmetrical $H_5O_2^+$-like bond can be easily enumerated by leaving that bond empty. There are four such oriented graphs, as shown in Figure 5. Initial guesses from two structures, those with all four waters hydrogen bound to the $H_5O_2^+$ unit symmetrically configured with respect to the $H_5O_2^+$ as double-acceptors, could be optimized to local minima with the proton localized symmetrically between two oxygens. The two

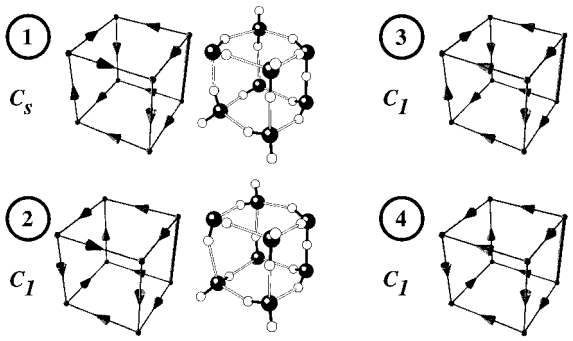

Figure 5. Oriented graphs and optimized structures for $H^+(H_2O)_8$ in which the excess proton resides in a symmetrical $H_5O_2^+$-like bond. The symmetry group of the graph is also indicated. Initial guesses from graphs **1** and **2** optimized to the local minima shown above. Structures **3** and **4** revert to the hydronium-like structure **1** in Figure 4 as the excess proton migrates toward the oxygen hydrogen bound to one double-donor and one double acceptor (upward as shown in the figure). Our attempts to optimize initial guesses based on **3** and **4** produced local minimum **1** of Figure 4.

structures, **3** and **4** in Figure 5, in which the four waters hydrogen bound to the $H_5O_2^+$ unit were not symmetrically configured, both optimized to the hydronium-like structure **1** in Figure 4. Both structures **3** and **4** in Figure 5 revert to structure **1** in Figure 4 by a slight deformation—migration of the excess proton toward the oxygen which is hydrogen bound to a double-acceptor and double-donor.

III. Dodecahedral $(H_2O)_{20}$ and $H^+(H_2O)_{20}$

Kassner and Hagen[75] first proposed that the abundance of protonated water clusters $(H_2O)_n$ near $n = 20$, 21 could be explained by dodecahedral clathrate structures. Since that time, dodecahedral clathrate structures have been invoked on numerous occasions to explain magic number phenomena in beam experiments.[3,11,76,77] The regularity of the geometrical structure, or even whether the hypothesized dodecahedral structure is actually present, has been debated in the literature. Plummer and Chen,[78] using the intermolecular potential of Stillinger and Rahman,[56] found that the dodecahedral cage was stable to 200 K in molecular dynamics simulations. Nagashima et al.[77] observed a defected dodecahedral cage surrounding a central ammonium ion in Monte Carlo simulations of $(H_2O)_{20}NH_4^+$. Kozack and Jordan,[21] using a potential model for $H^+(H_2O)_n$ in which a single proton was added as a distinct ionic species,[79] searched for minimum energy structures of $(H_2O)_{20}$, $H^+(H_2O)_{20}$, and $H^+(H_2O)_{21}$. They found that $H^+(H_2O)_{20}$ was most stable in a highly distorted clathrate, hardly recognizable as a dodecahedron. Khan investigated the stability of $(H_2O)_{20}$, $H^+(H_2O)_{20}$, and $H^+(H_2O)_{21}$ using the semiempirical ZINDO method, finding stable dodecahedral structures.[36,80] Smith and Dang studied low-energy structures and thermal properties of $Cs^+(H_2O)_{20}$ clusters.[22] They found that dodecahedral clathrates were unstable with respect to defected structures in which five-member rings were replaced pair a four- and six-membered ring. They interpreted their findings as an energy cost associated with adjacent double-acceptors or -donors, anticipating the trends we observe in a broader class of structures. Using density functional methods, Laasonen and Klein[81] found that dodecahedral $H^+(H_2O)_{21}$ was not a stable structure and that $H^+(H_2O)_{20}$ was either a highly defected dodecahedron or that the excess proton might be shared between two waters in the clathrate structure as an $H_5O_2^+$ unit and not as hydronium. On the other hand, it is difficult to explain the magic number abundance[82,83] of $H^+(H_2O)_{21}$ without invoking a favorable hydrogen-bonding arrangement such as the dodecahedral structure. At this time, it appears that the issue has not been settled definitively.

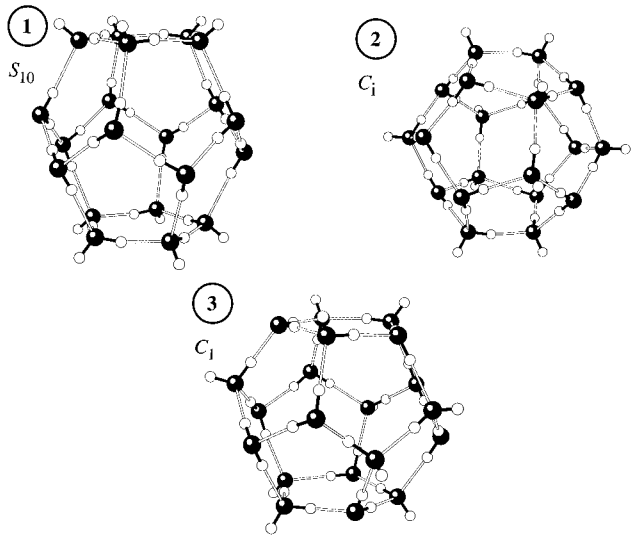

Figure 6. Lowest energy (**1**) S_{10}, (**2**) C_i, and overall lowest energy (**3**) C_1 structures for $(H_2O)_{20}$. The symmetry designation refers to the oriented graph which corresponds to the structure. The S_{10} structure **1** has 10 nearest neighbor double-donor (and, by topological constraints, 10 nearest neighbor double-acceptor) pairs, while the C_i structure **2** has 4 such pairs and C_1 structure **3** has only the minimum possible number of 3 such pairs. Both structures **2** and **3** have the maximum possible of six five-membered rings in which all the hydrogen bonds circulate in the same direction, while structure **1** has only two such rings.

Although it has long been recognized that many hydrogen-bonding arrangements are possible in water clathrates, their enumeration has never been attempted. Holland and Castleman[3] were aware that enumeration of the hydrogen-bonded arrangements were needed to discuss proton migration in the water clathrate at a statistical level, but concluded that "Due to the constraints on allowed configurations, counting the many permutations is a formidable problem." In this section we give the solution to this problem for dodecahedral $(H_2O)_{20}$ and $H^+(H_2O)_{20}$, with the latter holding the proton in either a hydronium or $H_5O_2^+$ unit.

A. $(H_2O)_{20}$. Using the counting algorithm described in eq 7, we have enumerated 30 026 oriented graphs corresponding to neutral $(H_2O)_{20}$. Very few have any symmetry: four have S_{10}, eight have C_5, 32 have C_i symmetry, and the remainder of the oriented graphs have no symmetry. We initially selected 99 configurations, those with symmetry or having the maximum number of five-membered rings in which the hydrogen bonds circulate in the same direction, which turned out to be six such rings. Using the OSS2 potential and with the initial guesses constructed in the same fashion as described for $(H_2O)_8$, 97 out of 99 initial guesses optimized to a structure corresponding to the original oriented graph, the remaining two configurations differed from the original one by flipping the direction of two hydrogen bonds.[84] Three of the optimized structures are shown in Figure 6.

The energy of these structures also appears to correlate with the same topological invariants as for cubic $(H_2O)_8$: an apparent repulsive interaction between nearest neighbor double-donors or double-acceptors and a weaker preference for rings of hydrogen bonds circulating in the same sense.

$$E(\mathrm{cm}^{-1}) = -69788.01 + 1246.64n_{2D-2D} - 231.203n_{5-\mathrm{ring}} \quad (28)$$

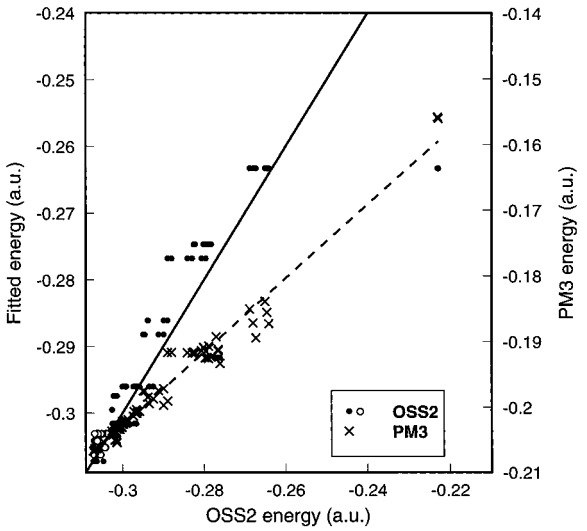

Figure 7. Comparison of the binding energies (relative to 20 free monomers) of different hydrogen-bonding arrangements of the dodecahedral clathrate $(H_2O)_{20}$ and a fit (eq 28) based on topological properties. Initially, 99 structures were optimized using the OSS potential[63] (filled symbols), starting from initial guesses based on oriented graphs selected from the full set of 30 026 for this structure. Perfect agreement between actual and fitted energies is indicated by the solid line in the figure. After fitting the energy of these 99 structures to obtain eq 28, the full set of 30 026 oriented graphs was screened to identify another 94 candidates for low-energy structures. The additional 94 initial guesses indeed optimized to very stable structures, indicated with open symbols in the figure. The crosses indicate the binding energy of clusters optimized using the PM3 semiempirical model. The PM3 optimizations used the same initial guesses as the OSS potential optimizations. The dashed line is a linear fit to the PM3 binding energy as a function of the OSS energy, provided as a guide to the eye confirming that the trends of the two models are similar.

A comparison of the actual binding energies (relative to 20 water monomers) and the energies predicted by the above fit to topological properties is given (filled symbols) in Figure 7. On the basis of a fit to these topological properties, an additional 94 structures were selected as likely candidates for low-energy structures. As confirmed in Figure 7 (open symbols), all these structures turned out to be very stable. The OSS2 model binding energy (relative to 20 free water molecules) of our most stable dodecahedral $(H_2O)_{20}$ structure was 9.64 kcal/mol per water molecule.

The energy difference between the least and most stable of the 99 + 94 structures we examined was 0.0843 au, or 52.9 kcal/mol, indicating that the hydrogen-bonding arrangement has considerable impact on the overall stability of these clathrates. It is not clear whether previous studies of dodecahedral clathrate structures[36,77,80,81] adequately searched through the many possible hydrogen-bonding arrangements. For example, we would predict that the structure pictured in Figure 1 of ref 81 would be a very unfavorable structure because it contains 10 nearest neighbor double-acceptor (and 10 nearest neighbor double-donor) pairs.

We also compared the predictions of the OSS2 potential[63] with the semiempirical PM3 method. The trends in the two models are in agreement, as there is a roughly linear relation between the OSS2 and PM3 energies (crosses and dotted line inFigure 7). However, the range of the PM3 energies is less than that of the OSS2 potential, the PM3 varying ~0.047 au or 29.7 kcal/mol between lowest and higher energy structure. This is to be expected, since the PM3 model is known to underestimate the binding energy in water clusters by roughly 30−40%.[63]

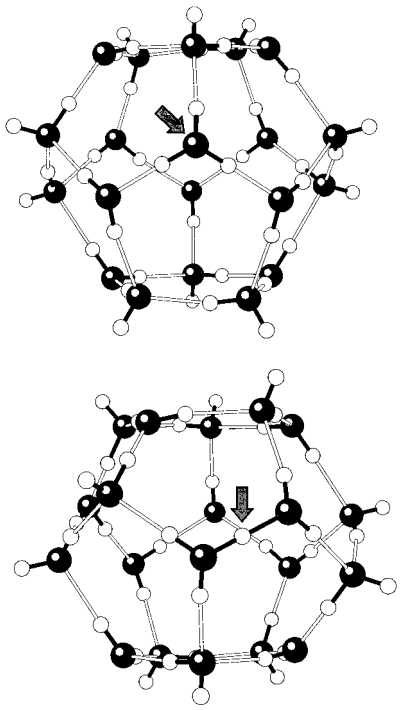

Figure 8. Examples of low-energy structures of $H^+(H_2O)_{20}$. The top figure is the lowest energy hydrogen-bonding arrangement found with the proton localized in a hydronium-like configuration. The bottom figure shows a local minimum in which the excess proton is shared between two water molecules in an $H_5O_2^+$-like arrangement. The arrows indicate the hydronium- or $H_5O_2^+$-like unit in each case.

B. $H^+(H_2O)_{20}$. We have considered two ways for a proton to add to a dodecahedral water cage, either as a triple-donor hydronium unit, for which there are 87 413 hydrogen-bonding topologies, or in a symmetrical $H_5O_2^+$ bond, for which 42 906 topologically distinct hydrogen-bonding arrangements are possible. In both cases, none of the oriented graphs have any symmetry. Study of double- or single-donating hydronium units is tractable with the methods developed here, but these structures were not considered in this work.

Of the 87 413 hydrogen-bonding topologies for $H^+(H_2O)_{20}$ containing a hydronium triple-donor, we selected 201 candidates for low-energy structures based on trends observed for $(H_2O)_8$, $H^+(H_2O)_8$, and neutral $(H_2O)_{20}$. [For a preliminary screening, we added a term $400n_{2A-Hyd}$ to eq 28.] Of the 201 initial guesses, 187 optimized to structures corresponding to the original oriented graph The most stable of these structures is shown in the top of Figure 8. In the remaining 14 of the original 201 guesses, one of the protons bound to the original hydronium unit migrated to a neighboring water during optimization, thereby shifting the position of the hydronium. The trend for avoidance of nearest neighbor double-donors and double-acceptors is obeyed in this data set: The eight lowest energy structures were precisely the eight with the minimum possible number of such bonds.

Equation 28 was used as a guide to select 163 candidates for low-energy structures from the 42 906 possible initial guesses for $H^+(H_2O)_{20}$ with the excess proton symmetrically disposed in an $H_5O_2^+$-like bond. In 10 of these cases, the excess proton clearly migrated to one side of the bond during optimization, leading to one of the 87 413 hydronium-containing structures. From all other initial guesses, the proton optimized to a structure that was between 2 and 10% from the midpoint, on average near 6%. In the example shown in the bottom of Figure 8, the excess proton is 6% from the midpoint between two oxygens.

There is an energy gap of roughly 2.3 kcal/mol favoring the lowest energy hydronium-like structures over the $H_5O_2^+$-like structures, in contrast to our results for $H^+(H_2O)_8$. The OSS2 model binding energy of our lowest energy $H^+(H_2O)_{20}$ (relative to 19 free waters and one H_3O^+) is 13.38 kcal/mol per oxygen.

IV. Discussion

Through advances in molecular beam and spectroscopic techniques, the range of water clusters open to detailed experimental study is rapidly expanding.[41−50] This has provided a rigorous testing ground for potential models of water, thereby enhancing our capability to model aqueous chemistry in, for example, biological or environmental applications. Interpreting these results depends upon accurate potential models and methods for enumerating cluster structures.

Analytic methods for the enumeration of cluster structures, like the one presented in this work, can complement and guide numerical techniques, especially for larger clusters in which the number of stable structures grows exponentially with cluster size. For example, we have shown that on the order of 3×10^4 local minima, corresponding to different hydrogen-bonding topologies, are to be expected for the dodecahedral clathrate $(H_2O)_{20}$. Presumably this information would be difficult to obtain numerically, and it would not be obvious when the numerical search exhausted all possible structures. Moreover, our enumeration of hydrogen-bonded arrangements can be used as input for statistical theories of cluster dynamics[3] for which this information has been previously lacking.

For the particular case of $(H_2O)_{20}$, we have found that approximately 50 kcal/mol separates the highest and lowest energy structures of a small subset of the $\sim 3 \times 10^4$ possible structures. Therefore it is not possible to reach conclusions about the relative stability of the clathrates relative to other structures without a representative sampling of possible hydrogen-bonding topologies, underscoring the need for enumeration techniques.

Enumeration of hydrogen-bonding topologies can be done for nonsymmetric structures, as well as the highly symmetrical cages treated here. For example, all possible hydrogen-bonding topologies for $(H_2O)_6$, the object of detailed experimental and theoretical study recently,[15,30,45] can be enumerated using the symmetric group of order 6!. We have done this exercise and found 1620 oriented graphs, of which 1392 are connected. Generating initial guesses for geometry optimization would be more difficult than for the symmetric cages studied in this work and has not been attempted here. A large set of candidates for optimization may facilitate subsequent numerical study.

Within several potential models, energetic trends can be correlated with cluster topology in the cubic and dodecahedral cages we have studied. The most significant trend is an energy cost associated with nearest neighbor double hydrogen bond donor or acceptor molecules. This leads us to derive a predictive expression for the stability of the cubic and dodecahedral water clusters. Using this we could see that there exists a class of particularly stable water dodecahedra. This suggests that consideration be given to the multitude of hydrogen-bonding topologies, first enumerated in this work, in calculations of the relative stability of the various forms of $(H_2O)_{20}$, $H^+(H_2O)_{20}$, and $H^+(H_2O)_{21}$. These trends and the enumeration techniques developed here provide guidance and a set of hypotheses for further testing with more sophisticated calculations on water clusters.

Acknowledgment. Early portions of this work were supported by NSF grant CHE-9115615 and by the Swedish Natural Science Research Council.

References and Notes

(1) Stillinger, F. H.; David, C. W. *J. Chem. Phys.* **1978**, *69*, 1473. David, C. W. *J. Chem. Phys.* **1980**, *73*, 3384. Stillinger, F. H.; Weber, T. A. *Chem. Phys. Lett.* **1981**, *79*, 259. Weber, T. A.; Stillinger, F. H. *J. Phys. Chem.* **1982**, *86*, 1314. Weber, T. A.; Stillinger, F. H. *J. Chem. Phys.* **1982**, *76*, 4028. Weber, T. A.; Stillinger, F. H. *J. Chem. Phys.* **1982**, *77*, 4150.
(2) Matsuoka, O.; Clementi, E.; Yoshimine, M. *J. Chem. Phys.* **1976**, *64* (4), 1351.
(3) Holland, P. M.; Castleman, A. W., Jr. *J. Chem Phys.* **1980**, *72* (11), 5984.
(4) Frisch, M. J.; Del Bene, J. E.; Binkley, J. S.; Schaefer, H. F., III. *J. Chem. Phys.* **1986**, *84* (4), 2279.
(5) Coker, D. F.; Miller, R. E.; Watts, R. O. *J. Chem. Phys.* **1980**, *82* (8), 3554.
(6) Belford, D. E.; Campbell, E. S. *J. Chem. Phys.* **1992**, *86* (12), 7013.
(7) Szalewicz, K.; Cole, S. J.; Kolos, W.; Bartlett, R. J. *J. Chem. Phys.* **1988**, *89* (6), 3662.
(8) Dykstra, C. E. *J. Chem. Phys.* **1989**, *91* (10), 6472.
(9) Smith, B. J.; Swanton, D. J.; Pople, J. A.; Schaefer, H. F., III. *J. Chem. Phys.* **1990**, *92* (2), 1240.
(10) Lee, E. F.; Dyke, J. M. *Mol. Phys.* **1991**, *73*, 375.
(11) Wei, S.; Shi, Z.; Castleman, A. W., Jr. *J. Chem. Phys.* **1991**, *94* (4), 3268.
(12) Knochenmuss, R.; Leutwyler, S. *J. Chem Phys.* **1992**, *96* (7), 5233.
(13) Feller, D. *J. Chem. Phys.* **1992**, *96* (8), 6104.
(14) Kim, K. S.; Mhin, B. J.; Choi, U. S.; Lee, K. *J. Chem. Phys.* **1992**, *97* (9), 6649.
(15) Mhin, B. J.; Kim, J.; Lee, S.; Lee, J. Y.; Kim, K. S. *J. Chem. Phys.* **1994**, *100*, 4484.
(16) Mó, O.; Yañez, M.; Elguero, J. *J. Chem. Phys.* **1992**, *97* (9), 6628.
(17) Wawak, R. J.; Wimmer, M. M.; Scheraga, H. A. *J. Phys. Chem.* **1992**, *96* (12), 5138.
(18) Schütz, M.; Bürgi, T.; Leutwyler, S.; Bürgi, H. B. *J. Chem. Phys.* **1993**, *99* (7), 5228; **1994**, *100* (2) 1780.
(19) Schütz, M.; Klopper, W.; Luthi, H. P.; Leutwyler, S. *J. Chem. Phys.* **1995**, *103* (14), 6114.
(20) Vegiri, A.; Farantos, S. C. *J. Chem. Phys.* **1993**, *98* (5), 4059.
(21) Kozack, R. E.; Jordan, P. C. *J. Chem. Phys.* **1993**, *99* (4), 2978.
(22) Smith, D. E.; Dang, L. X. *J. Chem. Phys.* **1994**, *101* (9), 7873.
(23) Tsai, C. J.; Jordan, K. D. *J. Chem. Phys.* **1995**, *95*, 3850.
(24) Laasonen, K.; Csajka, F.; Parrinello, M. *Chem. Phys. Lett.* **1992**, *194*, 172.
(25) Wales, D.; Ohmine, I. *J. Chem. Phys.* **1993**, *98* (9), 7245.
(26) Wales, D.; Ohmine, I. *J. Chem. Phys.* **1993**, *98* (9), 7256.
(27) Tsai, C. J.; Jordan, K. D. *J. Phys Chem.* **1993**, *97*, 5208.
(28) Tsai, C. J.; Jordan, K. D. *J. Phys. Chem.* **1993**, *97*, 11227.
(29) Tsai, C. J.; Jordan, K. D. *J. Chem. Phys.* **1993**, *99* (9), 6957.
(30) Tsai, C. J.; Jordan, K. D. *Chem. Phys. Lett.* **1993**, *213* (1,2), 181.
(31) Pedulla, J. M.; Vila, F.; Jordan, K. D. *J. Chem. Phys.* **1996**, *105* (24), 11091.
(32) Schenter, G.; Glendening, E. *J. Phys. Chem.* **1996**, *100*, 17152.
(33) Sremaniak, L. S.; Perera, L.; Berkowitz, M. L. *J. Chem Phys.* **1996**, *105* (9), 3715.
(34) Ojamäe, L.; Hermansson, K. *J. Phys Chem.* **1994**, *98*, 4271.
(35) Ojamäe, L.; Shavitt, I.; Singer, S. J. *Int. J. Quantum Chem.* **1995**, *29*, 657.
(36) Khan, A. *J. Phys. Chem.* **1995**, *99*, 12450.
(37) Khan, A. *Chem. Phys. Lett.* **1996**, *253*, 299.
(38) Khan, A. *Chem. Phys. Lett.* **1996**, *258*, 574.
(39) Khan, A. *J. Chem. Phys.* **1997**, *106* (13), 5537.
(40) Tuckerman, M. E.; Marx, D.; Klein, M. L.; Parrinello, M. *Science* **1997**, *275*, 817.
(41) Vernon, M. F.; Drajnovich, D. J.; Kwok, H. S.; Lisy, J. M.; Shen, Y. R.; Lee, Y. T. *J. Chem. Phys.* **1982**, *77* (1), 47.
(42) Pugliano, N.; Saykally, R. J. *J. Chem. Phys.* **1992**, *96* (3), 1832.
(43) Pugliano, N.; Cruzan, J. D.; Loeser, J. G.; Saykally, R. J. *J. Chem. Phys.* **1993**, *98* (9), 6600.
(44) Liu, Cruzan, and Liu, Cruzan, Saykally, R. *Science* **1996**, *271*, 929.
(45) Liu, K.; Brown, M. G.; Saykally, R. J.; Gregory, J. K.; Clary, D. C. *Nature* **1996**, *381*, 501.
(46) Bürgi, T.; Graf, S.; Leutwyler, S.; Klopper, W. *J. Chem. Phys.* **1995**, *103*, 1077.
(47) Klopper, W.; Schutz, M.; Luthi, H. P.; Leutwyler, S. *J. Chem. Phys.* **1995** *103* (3), 1077.
(48) Gregory, J. K.; Clary, D. C. *J. Chem. Phys.* **1995**, *102* (20), 7817.
(49) Gregory, J. K.; Clary, D. C.; Liu, K.; Brown, M. G.; Saykally, R. J. *Science* **1997**, *275*, 814.

(50) Dang, L. X.; Chang, T.-M. *J. Chem. Phys.* **1997**, *106* (19), 8149.
(51) Gruenloh, C. J.; Carney, J. R.; Arrington, C. A.; Zwier, T. S.; Fredericks, S. Y.; Jordan, K. D. *Science* **1997**, *276* (5319),1678.
(52) Berry, R. S. In *Few-Body Systems and Multiparticle Dynamics*; Proceedings of the Symposia of the Topical Group on Few-Body Systems and Multiparticle Dynamics, AIP Conf. No. 162, Micha, D. A., Ed.; AIP: New York, 1987; p 261.
(53) Beck, T. L.; Jellinek, J.; Berry, R. S. *J. Chem. Phys.* **1987**, *87*, 545.
(54) Landman, U.; Barnett, R. N.; Cleveland, C. L.; Luo, J.; Scharf, D.; Jortner, J. In *Few-Body Systems and Multiparticle Diynamics*; AIP Conference Proceedings, No. 162, Micha, D. A., Ed.; AIP: New York, 1987; p 200.
(55) Coe, J. V.; Saykally, R. J. In *Ion and Cluster Ion Spectroscopy and Structure*; Maier, J. P., Ed.; Elsevier: Amsterdam, 1989.
(56) Stillinger, F. H.; Rahman, A. *J. Chem. Phys.* **1974**, *60*, 1545.
(57) Belch, A. C.; Rice, S. A. *J. Chem. Phys.* **1987**, *86* (10), 5676.
(58) Corongiu, C.; Clementi, E. *J. Chem. Phys.* **1993**, *98* (3), 2241.
(59) Fletcher, N. H. *The Chemical Physics of Ice*; Cambridge: New York 1970.
(60) Hobbs, P. V. *Ice Physics*; Oxford: New York, 1974.
(61) Xie, Y.; Remington, R. B.; Schaefer, H. F., III. *J. Chem. Phys.* **1994**, *101* (6), 4878.
(62) Radhakrishnan, T. P.; Herndon, W. C. *J. Phys. Chem.* **1991**, *95*, 10609.
(63) Ojamäe, L.; Shavitt, I.; Singer, S. J. Manuscript in preparation.
(64) Stewart, J. J. P. *J. Comput. Chem.* **1989**, *10*, 209; **1989**, *10*, 221.
(65) Frisch, M. J.; Trucks, G. W.; Schlegel, H. B.; Gill, P. M. W.; Johnson, B. G.; Robb, M. A.; Cheeseman, J. R.; Keith, T.; Petersson, G. A.; Montgomery, J. A.; Raghavachari, K.; Al-Laham, M. A.; Zakrzewski, V. G.; Ortiz, J. V.; Foresman, J. B.; Peng, C. Y.; Ayala, P. Y.; Chen, W.; Wong, M. W.; Andres, J. L.; Replogle, E. S.; Gomperts, R.; Martin, R. L.; Fox, D. J.; Binkley, J. S.; Defrees, D. J.; Baker, J.; Stewart, J. P.; Head-Gordon, M.; Gonzalez, C.; Pople, J. A. *Gaussian94* (Revision B.3); Gaussian, Inc.: Pittsburgh, PA, 1995.
(66) Smith, D. E. Personal communication.
(67) Harary, F. *Michigan Math. J.* **1957**, *4*, 221.
(68) Harary, F.; Palmer, E. *Bull. Acad. Polon. Sci. Sér. Sci. Math. Astronom. Phys.* **1966**, *14*, 125.
(69) Harary, F.; Palmer, E. *Can. J. Math* **1966**, *18*, 853.
(70) Harary, F. *Graph theory*; Addison-Wesley: Reading, MA, 1969.
(71) Harary, F.; Palmer, E. M. *Graphical enumeration*; Academic, New York, 1973.
(72) Behzad, M.; Chartrand, G.; Lesniak-Foster, L. *Graphs and Digraphs*; Prindle, Weber and Schmidt: Boston, 1979.
(73) Wolfram, S. *Mathematica*; Wolfram Research: Champaign, IL, 1991.
(74) The initial guesses were rather crude. In this case, hydrogens participating in hydrogen bonds were placed 35% of the way along the oxygen−oxygen bond from the donor to the acceptor. The initial H−O−H angle was 90° for double donors and 125.3° for single donors.
(75) Kassner, J. L.; Hagen, D. E. *J. Chem. Phys.* **1976**, *64* (4), 1861.
(76) Shinohara, H.; Nagashima, U.; Tanaka, H.; Nishi, N. *J. Chem. Phys.* **1985**, *83* (8), 4183.
(77) Nagashima, U.; Shinohara, H.; Nishi, N.; Tanaka, H. *J. Chem. Phys.* **1986**, *84* (1), 209.
(78) Plummer, P. L. M.; Chen, T. S. *J. Phys. Chem.* **1983**, *87* (21), 4190.
(79) Kozack, R. E.; Jordan, P. C. *J. Chem. Phys.* **1993**, *96* (4), 3131.
(80) Khan, A. *Chem. Phys. Lett.* **1994**, *217* (4), 443.
(81) Laasonen, K.; Klein, M. L. *J. Phys. Chem.* **1994**, *98* (40), 10079.
(82) Magnera, T. F.; David, D. E.; Michl, J. *Chem. Phys. Lett.* **1991**, *182*, 363.
(83) Shi, Z.; Ford, J. V.; Wei, S.; Castleman, A. W., Jr. *J. Chem. Phys.* **1993**, *99* (3), 8009.
(84) Using the OSS2 model, we noted that it was possible to obtain additional structures, differing primarily in the OH bond lengths of certain water molecules. This deficiency of the potential was also noted in ref 63. However, in all such cases the energetic difference between such structures was exceedingly small, as was the energy barrier between the structures.